arXiv:1211.3132v1 [hep-ph] 13 Nov 2012

Double Parton Correlations in the Bag Model

Hsi-Ming Chang, Aneesh V. Manohar, and Wouter J. Waalewijn

Department of Physics, University of California at San Diego,
9500 Gilman Drive, La Jolla, CA 92093, U.S.A.

Double parton scattering is sensitive to correlations between the two partons in the hadron, including correlations in flavor, spin, color, momentum fractions and transverse separation. We obtain a first estimate of the size of these correlations by calculating the corresponding double parton distribution functions in a bag model of the proton. We find significant correlations between momentum fractions, spin and flavor, but negligible correlations with transverse separation. The model estimates of the relative importance of these correlations will help experimental studies disentangle them.

I. INTRODUCTION

High energy scattering processes such as Drell-Yan production, $pp \to \ell^+\ell^-$, are described by the scattering of two incoming partons, and the cross section is given by the convolution of a partonic scattering cross section $\hat\sigma$ and parton distribution functions (PDFs). Sometimes two hard partonic collisions take place within a single hadronic collision, a process which is known as double parton scattering (DPS). DPS is higher twist, i.e. it is suppressed by a power of $\Lambda^2_{\rm QCD}/Q^2$, where Q is the partonic center-of-mass energy of the collision. Despite this power suppression, the DPS scattering rate is still large enough that it has become a background for new physics searches at the LHC. For example, DPS contributes to same-sign WW and same-sign dilepton production [1–4], and is a background for Higgs studies in the channel $pp \to WH \to \ell\nu b\bar b$ [5–8]. DPS has been observed at the LHC; a preliminary study using $33\,{\rm pb}^{-1}$ of data found that 16% of the $W + 2$ jet events were due to DPS [9].

In the original work on DPS, the cross section was written as [10]

$$\mathrm{d}\sigma = \frac{1}{S}\sum_{i,j,k,l}\int \mathrm{d}^2\mathbf{z}_\perp\, F_{ij}(x_1,x_2,\mathbf{z}_\perp,\mu)F_{kl}(x_3,x_4,\mathbf{z}_\perp,\mu) \times \hat\sigma_{ik}(x_1x_3\sqrt{s},\mu)\hat\sigma_{jl}(x_2x_4\sqrt{s},\mu)\,. \qquad (1)$$

The double parton distribution function (dPDF) $F_{ij}(x_1,x_2,\mathbf{z}_\perp)$ describes the probability of finding two partons with flavors $i,j = g,u,\bar u,d,\dots$, longitudinal momentum fractions x_1,x_2 and transverse separation $\mathbf{z}_\perp$ inside the hadron. The partonic cross sections $\hat\sigma$ describe the short distance processes, and S is a symmetry factor that arises for identical particles in the final state. Eq. (1) ignores additional contributions that are sensitive to diparton correlations in flavor, spin and color, as well as parton-exchange interference contributions [11–14]. These correlations are present in QCD, and one of our goals is to estimate the size of these effects.

It is commonly assumed in DPS studies that the dependence on the transverse separation is uncorrelated with the momentum fractions or parton flavors,

$$F_{ij}(x_1,x_2,\mathbf{z}_\perp,\mu) = F_{ij}(x_1,x_2,\mu)G(\mathbf{z}_\perp,\mu)\,. \qquad (2)$$

In addition, a factorized ansatz is often made

$$F_{ij}(x_1,x_2,\mu) = f_i(x_1,\mu)f_j(x_2,\mu)\,\theta(1-x_1-x_2)(1-x_1-x_2)^n\,, \qquad (3)$$

where f denotes the usual (single) PDF. The factor $\theta(1-x_1-x_2)(1-x_1-x_2)^n$ smoothly imposes the kinematic constraint $x_1+x_2 \le 1$, and different values of the parameter $n > 0$ have been considered.

The dPDF is a nonperturbative function, but once it is known at a certain scale μ, its renormalization group evolution can be used to evaluate it at a different scale. The evolution of $F_{ij}(x_1,x_2,\mu)$ was determined a long time ago [15, 16]. It has recently been extended to include the $\mathbf{z}_\perp$ dependence and describe correlation and interference dPDFs [12–14, 17]. The color-correlated and interference dPDFs are all Sudakov suppressed at high energies [14, 18] and will therefore not be considered.

Eventually the dPDFs will be determined by fitting to experimental data, just as for the usual PDFs. Ref. [19] goes a step in this direction, showing how angular correlations in double Drell-Yan production may be used to study spin correlations in dPDFs. In this paper, we determine the dPDFs at a low scale $\mu \sim \Lambda_{\rm QCD}$ using a bag model for the proton [20]. This model calculation provides an estimate of the importance of various diparton correlations, which can be used to guide the experimental analysis. It also provides an estimate of dPDF distributions in the absence of more accurate determinations directly from experiment.

We follow some of the existing structure function calculations in the bag model [21–23]. There are obvious limitations to this approach, just as for bag model calculations of the usual PDFs. First of all, the bag model only describes valence quarks. Bag model calculations are only meaningful when the fields in the dPDF act inside the bag, which restricts the momentum fractions $x \gtrsim 1/(2MR) \sim 0.1$, where M is the proton mass and R is the bag radius. Finally, the bag was treated as rigid in the early literature, Ref. [21]. A consequence is that momentum is not conserved, and parton distributions do not vanish outside the physical region ($x > 1$). Alternative treatments of the bag were proposed to alleviate this problem [22–24]. We emphasize that we are not attempting to use the most sophisticated bag model description of the proton. Rather, we simply want to provide a first estimate of the size of the various correlation effects. Bag model PDFs are usually chosen as the initial value of PDFs at a low scale $\mu \sim \Lambda_{\mathrm{QCD}}$, which are then evolved to higher scales using their QCD evolution. Since in the bag model the valence quarks carry all the momentum, this initial scale μ needs to be taken quite low [22].

We also investigate Eqs. (2) and (3) in this paper, using our bag model results. We find that Eq. (2) holds reasonably well, but Eq. (3) is badly violated. Problems with Eq. (3) have already been pointed out in Ref. [25], using sum-rules and the evolution of the dPDF. In the simplest bag models of the type we consider, the color-correlated dPDFs F^T are given by $-2/3$ times the color-direct dPDFs F^1, since diquarks are in a $\overline{\mathbf{3}}$ representation of color.

II. CALCULATION

We briefly summarize the ingredients of the bag model [20] that are needed to calculate the dPDFs. The bag model wave functions are the solutions of the massless Dirac equation in a spherical cavity of radius R. We only need the ground state, which is given by

$$\Psi_m(\mathbf{r},t) = N \begin{pmatrix} j_0(\Omega|\mathbf{r}|/R)\ \chi_m \\ \mathrm{i}\,\hat{\mathbf{r}}\!\cdot\!\boldsymbol{\sigma}\, j_1(\Omega|\mathbf{r}|/R)\ \chi_m \end{pmatrix} e^{-\mathrm{i}\Omega t/R}\,, \tag{4}$$

for a bag centered at the origin. Here $\Omega = ER$,

$$N^2 = \frac{1}{R^3}\frac{\Omega^4}{\Omega^2 - \sin^2\Omega}\,, \quad \chi_m = \frac{1}{\sqrt{4\pi}}\begin{pmatrix}\delta_{m,\uparrow} \\ \delta_{m,\downarrow}\end{pmatrix}\,, \tag{5}$$

j_i are spherical Bessel functions, and $m = \uparrow, \downarrow$. The condition that the color current does not flow through the boundary $r^\mu \Psi \gamma_\mu T^A \Psi|_{|\mathbf{r}|=R} = 0$ leads to

$$j_0(\Omega) = j_1(\Omega) \quad \Rightarrow \quad \Omega \approx 2.043\,, \tag{6}$$

and we will take $R = 1.6$ fm in our numerical analysis.

The quark field is expanded in terms of bag wave functions, quark creation and annihilation operators $a_i(\mathbf{a})$, $a_i^\dagger(\mathbf{a})$ and antiquark creation and annihilation operators $b_i(\mathbf{a})$, $b_i^\dagger(\mathbf{a})$. These operators create or annihilate quarks and antiquarks in a bag centered at $\mathbf{r} = \mathbf{a}$ [see Eq. (14)]. We only need the operators for the ground state wave functions in Eq. (4) with $m = \uparrow, \downarrow$.

The spin-up proton wave function is given in terms of the standard quark model wave functions as

$$\frac{1}{\sqrt{6}}|uud\rangle\,(2|\uparrow\uparrow\downarrow\rangle - |\uparrow\downarrow\uparrow\rangle - |\downarrow\uparrow\uparrow\rangle)\,. \tag{7}$$

As usual, the color indices are suppressed, and the wave function has to be symmetrized over permutations. Ignoring color, one can also write the wave function in terms of bosonic [26] creation operators,

$$\begin{aligned}|P\uparrow, \mathbf{r} = \mathbf{a}\rangle = \frac{1}{\sqrt{3}}\Big[&a^\dagger_{u\uparrow}(\mathbf{a})a^\dagger_{u\uparrow}(\mathbf{a})a^\dagger_{d\downarrow}(\mathbf{a}) \\ &- a^\dagger_{u\uparrow}(\mathbf{a})a^\dagger_{u\downarrow}(\mathbf{a})a^\dagger_{d\uparrow}(\mathbf{a})\Big]|0, \mathbf{r} = \mathbf{a}\rangle\,.\end{aligned} \tag{8}$$

Here $|P\uparrow, \mathbf{r} = \mathbf{a}\rangle$ and $|0, \mathbf{r} = \mathbf{a}\rangle$ are the proton and empty bag state, respectively, both at position $\mathbf{a}$. The $a^\dagger_{qm}(\mathbf{a})$ denotes the creation operator for a quark of flavor q with spin m in a bag at position $\mathbf{a}$.

An important difference between various calculations in the literature is the treatment of the overlap between empty bags at different positions,

$$\begin{aligned}&\langle 0, \mathbf{r} = \mathbf{a}|0, \mathbf{r} = \mathbf{b}\rangle = \delta^3(\mathbf{a} - \mathbf{b}) &&\text{in Ref. [21]}\,, \\ &\langle 0, \mathbf{r} = \mathbf{a}|0, \mathbf{r} = \mathbf{b}\rangle = 1 &&\text{in Refs. [22, 23]}\,.\end{aligned} \tag{9}$$

These opposite limits treat the bags as either completely rigid or fully flexible, and the latter will be our default. We will return to the rigid bag in Sec. II D. To account for the displacement between bags, we follow Ref. [22] in taking

$$\{a_i(\mathbf{a}), a_j^\dagger(\mathbf{b})\} = \delta_{ij}\int \mathrm{d}^3x\, \Psi_j^\dagger(\mathbf{x} - \mathbf{b})\Psi_i(\mathbf{x} - \mathbf{a})\,. \tag{10}$$

For the rigid bag these are replaced by the familiar anticommutation relations

$$\{a_i, a_j^\dagger\} = \delta_{ij}\,, \tag{11}$$

where we only need the relation when a and $a^\dagger$ are at the same bag position, because of Eq. (9).

The proton state with momentum $\mathbf{p}$ is constructed using the Peierls-Yoccoz (PY) projection [27],

$$|P, \mathbf{p}\rangle = \frac{1}{\phi_3(\mathbf{p})}\int \mathrm{d}^3\mathbf{a}\, e^{\mathrm{i}\mathbf{a}\cdot\mathbf{p}}\,|P, \mathbf{r} = \mathbf{a}\rangle\,, \tag{12}$$

where $\phi_3(\mathbf{p})$ fixes the (non-relativistic) normalization of the state. The functions $\phi_n(\mathbf{p})$ are given by

$$|\phi_n(\mathbf{p})|^2 = \int \mathrm{d}\mathbf{a}\, e^{-\mathrm{i}\mathbf{p}\cdot\mathbf{a}}\Big[\int \mathrm{d}\mathbf{x}\, \Psi^\dagger(\mathbf{x} - \mathbf{a})\Psi(\mathbf{x})\Big]^n\,, \tag{13}$$

which we will need for $n = 1, 2, 3$.

The final ingredient is the expression for quark fields acting in the bag. The field for a u-quark relative to a bag at $\mathbf{a}$ is given by [22]

$$u(\mathbf{x}, t) = \sum_{m=\uparrow,\downarrow} a_{um}(\mathbf{a})\Psi_m(\mathbf{x} - \mathbf{a})e^{-\mathrm{i}\Omega t/R} + \dots\,. \tag{14}$$

Here "…" denotes contributions from other bag states that will not be needed[1]. The expression for d-quarks is similar.

---

[1] We will not consider the so-called z-graph or four-quark intermediate state contribution [21, 23], where the field creates an antiquark. This only contributes at small x and is thus outside the range of validity of the calculation.

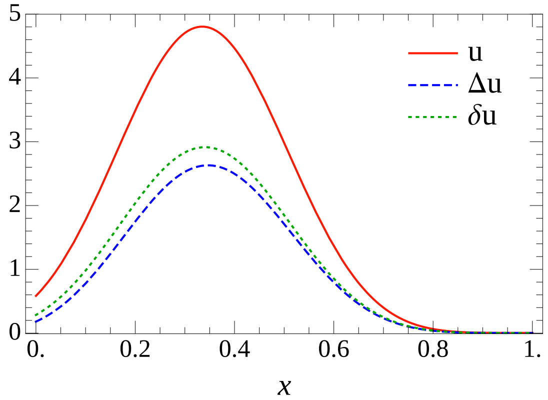

FIG. 1. The proton PDFs u (solid red), Δu (dashed blue) and δu (dotted green).

A. Single PDF

We first summarize the well-known calculation of the (single) PDF in the bag model. The light-cone vectors are

$$n^\mu = (1,0,0,1)\,, \qquad \bar{n}^\mu = (1,0,0,-1)\,, \tag{15}$$

and we assume the light-cone gauge $n\cdot A = 0$. In the proton rest frame, where $p^\mu = (M,\mathbf{0})$,[2]

$$\begin{aligned} q(x) &= 2M \int \frac{\mathrm{d}z^+}{4\pi}\, e^{-\mathrm{i}xMz^+/2} \\ &\quad \times \Big\langle P,\mathbf{p}=\mathbf{0}\Big|\bar{q}\Big(z^+\frac{\bar{n}}{2}\Big)\frac{\not{\bar{n}}}{2}\, q(0)\Big|P,\mathbf{p}=\mathbf{0}\Big\rangle \\ &= \sum_{m_1,m_2=\uparrow,\downarrow} \big\langle P,\mathbf{r}=\mathbf{0}\big|a^\dagger_{qm_1}(\mathbf{0})a_{qm_2}(\mathbf{0})\big|P,\mathbf{r}=\mathbf{0}\big\rangle \\ &\quad \times \frac{2M}{(2\pi)^2}\int_{|\Omega/R-xM|}^{\infty} \mathrm{d}|\mathbf{k}|\,|\mathbf{k}|\,\bar{\Psi}_{m_1}(\mathbf{k})\frac{\not{\bar{n}}}{2}\Psi_{m_2}(\mathbf{k})\frac{|\phi_2(\mathbf{k})|^2}{|\phi_3(0)|^2}\,. \end{aligned} \tag{16}$$

The factor of $2M$ is due to the nonrelativistic normalization of states, and ϕ_2 is given by Eq. (13). The delta function sets

$$k^z = \frac{\Omega}{R} - xM\,. \tag{17}$$

In using Eq. (14) we assumed that the field $\bar{q}$ acts at the position of the bag of the left state and q at the position of the bag of the right state [22]. The third line of Eq. (16) contains all the dependence on the spin-flavor wave function of Eq. (7), which is connected with the spin of the bag wave functions through the sum on $m_{1,2}$. For the unpolarized PDF only $m_1 = m_2$ contributes, and the matrix element simply counts the number of quarks of a given flavor q in the proton,

$$n_q = \sum_{m=\uparrow,\downarrow} \big\langle P,\mathbf{r}=\mathbf{0}\big|a^\dagger_{qm}(\mathbf{0})a_{qm}(\mathbf{0})\big|P,\mathbf{r}=\mathbf{0}\big\rangle\,. \tag{18}$$

An immediate implication of Eq. (16) is that the peak of q is located at $x = \Omega/(MR)$, independent of the quark flavor. This disagreement with experimental measurements of u and d may be alleviated by refining the bag model, see e.g. Ref. [28]. We will restrict ourselves to the simplest bag models in this paper, so its limitations should be be kept in mind while using the results.

The extension of Eq. (16) to longitudinal and transversely polarized quark distributions is given by replacing $\frac{\not{\bar{n}}}{2}$ by $\frac{\not{\bar{n}}}{2}\gamma_5$ for Δq and $\frac{\not{\bar{n}}}{2}\gamma_\perp^\mu\gamma_5$ for δq. Δq and δq only contribute in processes involving longitudinally and transversely polarized protons, respectively. The matrix elements required are evaluated in Sec. II C. To aid the evaluation of the remaining integral in Eq. (16), convenient expressions for the functions ϕ_i and the bag wave function in momentum space are given in Appendix A. The resulting distributions for the various proton PDFs are compared in Fig. 1.

B. Double PDF

We calculate the double PDF using the definitions in Ref. [14]. We will not consider color correlated or interference double PDF, since these are Sudakov suppressed. Starting with the spin-averaged dPDF $F_{q_1q_2}(x_1,x_2,\mathbf{k}_\perp)$

$$\begin{aligned} F_{q_1q_2}(x_1,x_2,\mathbf{k}_\perp) &= -8\pi M^2 \int \mathrm{d}^2\mathbf{z}_\perp\, e^{-\mathrm{i}\mathbf{z}_\perp\cdot\mathbf{k}_\perp} \int \frac{\mathrm{d}z_1^+}{4\pi}\frac{\mathrm{d}z_2^+}{4\pi}\frac{\mathrm{d}z_3^+}{4\pi} e^{-\mathrm{i}x_1Mz_1^+/2}\, e^{-\mathrm{i}x_2Mz_2^+/2}\, e^{\mathrm{i}x_1Mz_3^+/2} \\ &\quad \times \Big\langle P,\mathbf{p}=\mathbf{0}\Big|\Big[\bar{q}_1\Big(z_1^+\frac{\bar{n}}{2}\Big)\frac{\not{\bar{n}}}{2}\Big]_c\Big[\bar{q}_2\Big(z_2^+\frac{\bar{n}}{2}+z_\perp\Big)\frac{\not{\bar{n}}}{2}\Big]_d q_{1,c}\Big(z_3^+\frac{\bar{n}}{2}+z_\perp\Big)q_{2,d}(0)\Big|P,\mathbf{p}=\mathbf{0}\Big\rangle \\ &= \sum_{m_1,m_2,m_3,m_4} \big\langle P,\mathbf{r}=\mathbf{0}\big|a^\dagger_{q_1m_1}(\mathbf{0})a^\dagger_{q_2m_2}(\mathbf{0})a_{q_2m_4}(\mathbf{0})a_{q_1m_3}(\mathbf{0})\big|P,\mathbf{r}=\mathbf{0}\big\rangle \end{aligned} \tag{19}$$

---

[2] We also use the notation q for the PDF f_q, and qq, $q\Delta q$, … for the dPDFs F_{qq}, $F_{q\Delta q}$, ….

$$\times\, 8\pi\, M^2 \int \frac{\mathrm{d}\mathbf{k}_1}{(2\pi)^3}\, \frac{\mathrm{d}\mathbf{k}_2}{(2\pi)^3}\, \frac{\mathrm{d}\mathbf{k}_3}{(2\pi)^3}\, \delta\Big(x_1 M - \frac{\Omega}{R} + \mathbf{k}_{1z}\Big)\, \delta\Big(x_2 M - \frac{\Omega}{R} + \mathbf{k}_{2z}\Big)\, \delta\Big(x_1 M - \frac{\Omega}{R} + \mathbf{k}_{3z}\Big)$$
$$\times\, (2\pi)^2 \delta^2(\mathbf{k}_{1\perp} - \mathbf{k}_{3\perp} - \mathbf{k}_\perp)\, \bar{\Psi}_{m_1}(\mathbf{k}_1) \frac{\not{\bar{n}}}{2} \Psi_{m_3}(\mathbf{k}_3)\, \bar{\Psi}_{m_2}(\mathbf{k}_2) \frac{\not{\bar{n}}}{2} \Psi_{m_4}(\mathbf{k}_1 + \mathbf{k}_2 - \mathbf{k}_3) \frac{|\phi_1(\mathbf{k}_1 + \mathbf{k}_2)|^2}{|\phi_3(0)|^2}\,,$$

where ϕ_1 is given by Eq. (13). Results for the matrix elements on the third line of Eq. (19) are given in Sec. II C. The expressions in Appendix A aid an efficient evaluation of the remaining integrals. The numerical integrals were performed using the CUBA integration package [29].

C. Spin Correlations

The computation of spin-correlated double PDFs is almost identical to Eq. (19). The spinors $\frac{\not{\bar{n}}}{2} \otimes \frac{\not{\bar{n}}}{2}$ in Eq. (19) are replaced by [12–14]

$F_{\Delta q_1 \Delta q_2}$	$\frac{\not{\bar{n}}}{2}\gamma_5 \otimes \frac{\not{\bar{n}}}{2}\gamma_5$
$M\lvert\mathbf{z}_\perp\rvert\, F_{q_1 \delta q_2}$	$-\frac{1}{\lvert\mathbf{z}_\perp\rvert}\, \frac{\not{\bar{n}}}{2} \otimes \frac{\not{\bar{n}}}{2}\, \gamma_\perp^\mu \epsilon_{\mu\nu} z_\perp^\nu$
$M\lvert\mathbf{z}_\perp\rvert\, F_{\Delta q_1 \delta q_2}$	$\frac{1}{\lvert\mathbf{z}_\perp\rvert}\, \frac{\not{\bar{n}}}{2}\gamma_5 \otimes \frac{\not{\bar{n}}}{2}\, \not{z}_\perp \gamma_5$
$F_{\delta q_1 \delta q_2}$	$\frac{\not{\bar{n}}}{2}\gamma_\perp^\mu \gamma_5 \otimes \frac{\not{\bar{n}}}{2}\gamma_\mu^\perp \gamma_5$
$M^2\lvert\mathbf{z}_\perp\rvert^2\, F^t_{\delta q_1 \delta q_2}$	$\frac{2}{\lvert\mathbf{z}_\perp\rvert^2}\big(z_\perp^\mu z_\perp^\nu + \frac{1}{2}\mathbf{z}_\perp^2 g_\perp^{\mu\nu}\big)\frac{\not{\bar{n}}}{2}\gamma_\mu \gamma_5 \otimes \frac{\not{\bar{n}}}{2}\gamma_\nu \gamma_5$

We have multiplied the dPDFs by appropriate factors of $M|\mathbf{z}_\perp|$ to remove explicit dependence on $|\mathbf{z}_\perp|$ and M from the spin structure. These will be the quantities that we plot. As in Eq. (19), we again switch to Fourier space. Azimuthal symmetry implies that we may simply pick $\mathbf{k}_\perp$ to be along the 1 direction, resulting in the γ-matrix structures:

$M\lvert\mathbf{z}_\perp\rvert\, F_{q_1 \delta q_2}$	$\frac{\not{\bar{n}}}{2} \otimes \frac{\not{\bar{n}}}{2}\gamma^2$
$M\lvert\mathbf{z}_\perp\rvert\, F_{\Delta q_1 \delta q_2}$	$-\frac{\not{\bar{n}}}{2}\gamma_5 \otimes \frac{\not{\bar{n}}}{2}\gamma^1 \gamma_5$
$F_{\delta q_1 \delta q_2}$	$-\frac{\not{\bar{n}}}{2}\gamma^1 \gamma_5 \otimes \frac{\not{\bar{n}}}{2}\gamma^1 \gamma_5 - \frac{\not{\bar{n}}}{2}\gamma^2 \gamma_5 \otimes \frac{\not{\bar{n}}}{2}\gamma^2 \gamma_5$
$M^2 \mathbf{z}_\perp^2\, F^t_{\delta q_1 \delta q_2}$	$\frac{\not{\bar{n}}}{2}\gamma^1 \gamma_5 \otimes \frac{\not{\bar{n}}}{2}\gamma^1 \gamma_5 - \frac{\not{\bar{n}}}{2}\gamma^2 \gamma_5 \otimes \frac{\not{\bar{n}}}{2}\gamma^2 \gamma_5$

The spin structures $q_1 \delta q_2$ and $\Delta q_1 \delta q_2$ vanish in our calculation. This follows from the factorized form of the dPDF in Eq. (19), where only $\phi_1(\mathbf{k}_1 + \mathbf{k}_2)$ introduces correlations between $\mathbf{k}_1$ and $\mathbf{k}_2$. Specifically, this allows one to perform different reflections on each momentum, $\mathbf{k}_{1x} \to |\mathbf{k}_\perp| - \mathbf{k}_{1x}$ and $\mathbf{k}_{2x} \to -|\mathbf{k}_\perp| - \mathbf{k}_{2x}$, under which the integrand is odd. Though this is due to the form of the bag model matrix elements, it suggests that the spin structures $q_1 \delta q_2$ and $\Delta q_1 \delta q_2$ are likely smaller than the others.

We now evaluate the spin-flavor matrix elements that enter in the single and double PDFs. Since we suppressed the *antisymmetric* color wave function of the proton, the creation and annihilation operators essentially satisfy *commutation* relations. For the unpolarized and longitudinally polarized single PDF only $m_1 = m_2$ contributes, and we find the weighting:

q m	$\langle P \uparrow \lvert a^\dagger_{qm} a_{qm} \rvert P \uparrow \rangle$
$u \uparrow$	5/3
$u \downarrow$	1/3
$d \uparrow$	1/3
$d \downarrow$	2/3

For δq we need a transversely polarized proton

$$|P \rightarrow\rangle = \frac{1}{\sqrt{2}}(|P \uparrow\rangle + |P \downarrow\rangle)\,. \tag{20}$$

The non-vanishing matrix elements are

q	m_1	m_2	$\langle P \rightarrow \lvert a^\dagger_{qm_1} a_{qm_2} \rvert P \rightarrow \rangle$
u	$\uparrow$	$\downarrow$	2/3
u	$\downarrow$	$\uparrow$	2/3
d	$\uparrow$	$\downarrow$	-1/6
d	$\downarrow$	$\uparrow$	-1/6

The double PDFs we consider are invariant under spin flip (they are only sensitive to diparton spin correlations), so we can simply use a spin-up proton. The nonvanishing matrix elements are

q_1	q_2	m_1	m_2	m_3	m_4	$\langle P \uparrow \lvert a^\dagger_{q_1 m_1} a^\dagger_{q_2 m_2} a_{q_2 m_4} a_{q_1 m_3} \rvert P \uparrow \rangle$
u	u	$\uparrow$	$\uparrow$	$\uparrow$	$\uparrow$	4/3
u	u	$\uparrow$	$\downarrow$	$\uparrow$	$\downarrow$	1/3
u	u	$\downarrow$	$\uparrow$	$\downarrow$	$\uparrow$	1/3
u	u	$\uparrow$	$\downarrow$	$\downarrow$	$\uparrow$	1/3
u	u	$\downarrow$	$\uparrow$	$\uparrow$	$\downarrow$	1/3
u	d	$\uparrow$	$\uparrow$	$\uparrow$	$\uparrow$	1/3
u	d	$\uparrow$	$\downarrow$	$\uparrow$	$\downarrow$	4/3
u	d	$\downarrow$	$\uparrow$	$\downarrow$	$\uparrow$	1/3
u	d	$\uparrow$	$\downarrow$	$\downarrow$	$\uparrow$	-2/3
u	d	$\downarrow$	$\uparrow$	$\uparrow$	$\downarrow$	-2/3

Note that due to these spin-flavor correlations, the dPDF for *uu* and *ud* do not simply differ by an overall factor, as is the case for the single PDF.

D. Rigid Bag

For a rigid bag, the overlap of empty bag states is

$$\langle 0, \mathbf{r} = \mathbf{a} | 0, \mathbf{r} = \mathbf{b} \rangle = \delta^3(\mathbf{a} - \mathbf{b})\,. \tag{21}$$

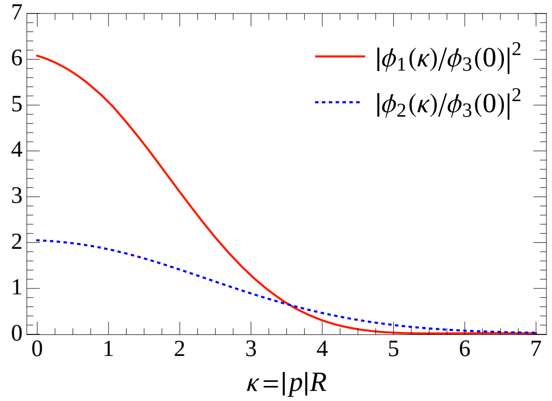

FIG. 2. Plot of the PY factors which enter the calculation of the single PDF (dotted blue) and double PDF (solid red). They suppress the PDFs in the unphysical regions $x > 1$ and $x < 0$.

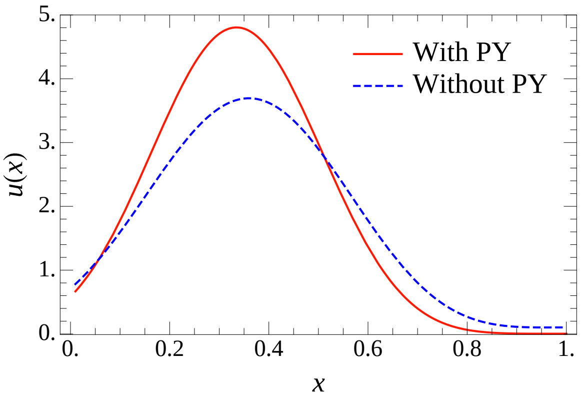

FIG. 3. Plot of the bag model proton PDF $u(x)$ with (solid red) and without (dotted blue) PY factors.

The only change to the single PDF in Eq. (16) is that it removes the PY factor $|\phi_2(\mathbf{k})|^2/|\phi_3(\mathbf{0})|^2$. This factor suppresses the "leakage" of the PDF into the unphysical regions $x < 0$ and $x > 1$, without affecting the integral over all x, see Sec. II E. The PY factor is plotted in Fig. 2, and the PDF with and without the PY factor is shown in Fig. 3.

Similarly, the rigid bag overlap in Eq. (21) removes the factor $|\phi_1(\mathbf{k})|^2/|\phi_3(\mathbf{0})|^2$ (also plotted in Fig. 2) from the double PDF in Eq. (19). In this case the double PDF factors and there are no correlations between the momentum fractions x_1 and x_2, which is a clear shortcoming of treating the bag as rigid. At $\mathbf{k}_\perp = \mathbf{0}$ the rigid bag dPDF takes a particularly simple form

$$F_{q_1 q_2}(x_1, x_2, \mathbf{k}_\perp = \mathbf{0}) = \frac{c_{q_1 q_2}}{n_{q_1} n_{q_2}}\, q_1(x_1) q_2(x_2)\,, \qquad (22)$$

where the coefficient $c_{q_1 q_2}$ is fixed by the spin-flavor wave function

$$c_{q_1 q_2} = \sum_{m_1=m_3, m_2=m_4} \big\langle P, \mathbf{r}=\mathbf{0} \big| a^\dagger_{q_1 m_1}(\mathbf{0}) a^\dagger_{q_2 m_2}(\mathbf{0}) \\ \times a_{q_2 m_4}(\mathbf{0}) a_{q_1 m_3}(\mathbf{0}) \big| P, \mathbf{r}=\mathbf{0} \big\rangle\,. \qquad (23)$$

From the tables in Sec. II C, we find that $c_{uu} = c_{ud} = 2$.

E. Normalization

The normalization of the single PDF and double PDF is given by integrating over all x, including unphysical regions. Both treatments of the bag in Eq. (9) will be considered. The single PDF in a rigid bag gives

$$\begin{aligned} \int \mathrm{d}x\, q(x) &= n_q \int \mathrm{d}x\, \frac{2M}{(2\pi)^2} \int_{|xM-\Omega/R|}^\infty \mathrm{d}|\mathbf{k}|\, |\mathbf{k}|\, \bar\Psi_m(\mathbf{k}) \frac{\not{\bar{n}}}{2} \Psi_m(\mathbf{k}) \\ &= 2n_q \int \frac{\mathrm{d}^3\mathbf{k}}{(2\pi)^3}\, \Psi^\dagger(\mathbf{k}) \frac{\not{n}\not{\bar{n}}}{4} \Psi(\mathbf{k}) \\ &= n_q \int \mathrm{d}^3\mathbf{y}\, |\Psi(\mathbf{y})|^2 \\ &= n_q\,. \end{aligned} \qquad (24)$$

Here we used that

$$\gamma^0 \frac{\not{\bar{n}}}{2} = \frac{\not{n}\not{\bar{n}}}{4}\,, \qquad \frac{\not{n}\not{\bar{n}}}{4} + \frac{\not{\bar{n}}\not{n}}{4} = 1\,. \qquad (25)$$

This second equation and the symmetry between n and $\bar{n}$ implies that we could replace $\not{n}\not{\bar{n}}/4 \to 1/2$ in Eq. (24). The corresponding calculation with a flexible bag, i.e. including the PY factor, is

$$\begin{aligned} &\int \mathrm{d}x\, q(x) \\ &= \frac{2Mn_q}{(2\pi)^2} \int \mathrm{d}x \int_{|xM-\Omega/R|}^\infty \mathrm{d}|\mathbf{k}|\, |\mathbf{k}|\, \bar\Psi_m(\mathbf{k}) \frac{\not{\bar{n}}}{2} \Psi_m(\mathbf{k}) \frac{|\phi_2(\mathbf{k})|^2}{|\phi_3(0)|^2} \\ &= \frac{2n_q}{|\phi_3(0)|^2} \int \frac{\mathrm{d}^3\mathbf{k}}{(2\pi)^3}\, \Psi^\dagger_m(\mathbf{k}) \frac{\not{n}\not{\bar{n}}}{4} \Psi_m(\mathbf{k})\, |\phi_2(\mathbf{k})|^2 \\ &= \frac{n_q}{|\phi_3(0)|^2} \int \frac{\mathrm{d}^3\mathbf{k}}{(2\pi)^3} \int \mathrm{d}^3\mathbf{x}_1\, \mathrm{d}^3\mathbf{y}_1\, e^{\mathrm{i}\mathbf{k}\cdot\mathbf{x}_1}\, \Psi^\dagger(\mathbf{y}_1 - \mathbf{x}_1) \Psi(\mathbf{y}_1) \\ &\quad \times \int \mathrm{d}^3\mathbf{x}_2\, e^{-\mathrm{i}\mathbf{k}\cdot\mathbf{x}_2} \Big[\int \mathrm{d}\mathbf{y}_2\, \Psi^\dagger(\mathbf{y}_2 - \mathbf{x}_2) \Psi(\mathbf{y}_2) \Big]^2 \\ &= n_q\,, \end{aligned} \qquad (26)$$

and has the same normalization. However, the PY factor reduces the PDF at unphysical x. Specifically, 2% of the contribution to the integral in Eq. (26) is from the unphysical region, compared to 11% in Eq. (24).

For the double PDF, the normalization for the rigid bag follows from Eqs. (22) and (24)

$$\begin{aligned} &\int \mathrm{d}x_1\, \mathrm{d}x_2\, \mathrm{d}\mathbf{z}_\perp F_{q_1 q_2}(x_1, x_2, \mathbf{z}_\perp) \\ &\quad = \frac{c_{q_1 q_2}}{n_{q_1} n_{q_2}} \int \mathrm{d}x_1\, \mathrm{d}x_2\, q_1(x_1) q_2(x_2) \\ &\quad = c_{q_1 q_2}\,, \end{aligned} \qquad (27)$$

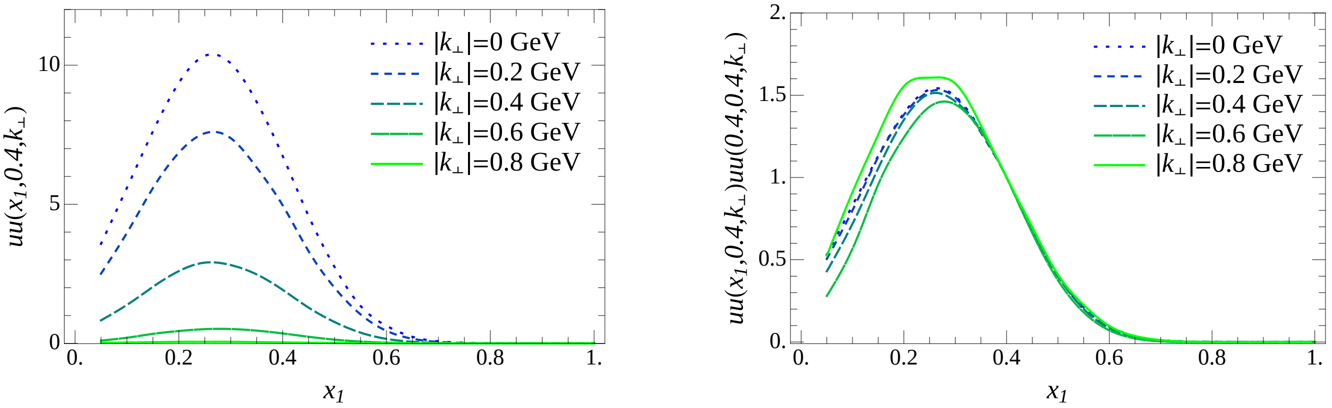

FIG. 4. The double PDF $uu(x_1, x_2, \mathbf{k}_\perp)$ as a function of x_1 and $|\mathbf{k}_\perp|$ for fixed $x_2 = 0.4$. The right panel tests the ansatz in Eq. (2) that x_i and $\mathbf{k}_\perp$ are uncorrelated. This holds reasonably well, since the different $|\mathbf{k}_\perp|$ curves are nearly identical.

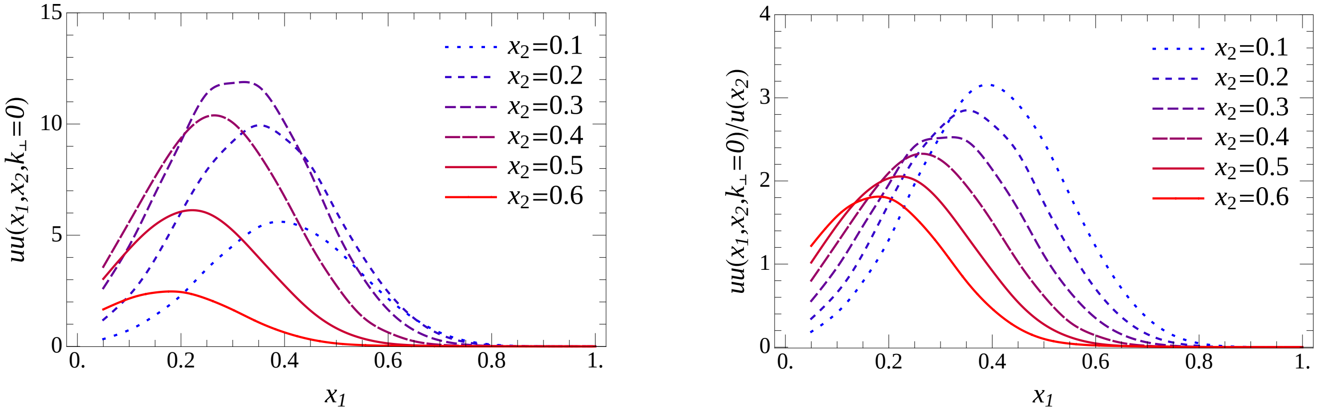

FIG. 5. The double PDF $uu(x_1, x_2, \mathbf{k}_\perp)$ as a function of x_1 and x_2 for fixed $\mathbf{k}_\perp = \mathbf{0}$. In the right panel we divide by $u(x_2)$ to test the often used assumption in Eq. (3) that the x_i are uncorrelated. This clearly fails, since the ratio depends strongly on x_2.

where the coefficient $c_{q_1 q_2}$ is given in Eq. (23). The calculation including the PY factor is similar to Eq. (26)

$$\begin{aligned}\int & \mathrm{d}x_1\, \mathrm{d}x_2\, \mathrm{d}^2\mathbf{z}_\perp F_{qq}(x_1, x_2, \mathbf{z}_\perp) \\ & = 4 c_{q_1 q_2} \int \frac{\mathrm{d}^3\mathbf{k}_1}{(2\pi)^3} \frac{\mathrm{d}^3\mathbf{k}_2}{(2\pi)^3}\, \Psi^\dagger(\mathbf{k}_1) \frac{\not{n}\not{\bar{n}}}{4} \Psi(\mathbf{k}_1) \\ & \times \Psi^\dagger(\mathbf{k}_2) \frac{\not{n}\not{\bar{n}}}{4} \Psi(\mathbf{k}_2)\, \frac{|\phi_1(\mathbf{k}_1 + \mathbf{k}_2)|^2}{|\phi_3(0)|^2} \\ & = c_{q_1 q_2} [1 + \mathcal{O}(< 1\%)]\,. \end{aligned} \tag{28}$$

The small correction with respect to Eq. (27) arises because we can no longer replace $\not{n}\not{\bar{n}}/4 \to 1/2$. Specifically, Eq. (A1) implies

$$\begin{aligned}\Psi^\dagger(\mathbf{k}) \frac{\not{n}\not{\bar{n}}}{4} \Psi(\mathbf{k}) &= \frac{\pi R^3 \Omega^2}{2(\Omega^2 - \sin^2\Omega)} (s_1^2 + 2 s_1 s_2 \hat{\mathbf{k}}_z + s_2^2)\,, \\ \Psi^\dagger(\mathbf{k}) \Psi(\mathbf{k}) &= \frac{\pi R^3 \Omega^2}{(\Omega^2 - \sin^2\Omega)} (s_1^2 + s_2^2) \end{aligned} \tag{29}$$

Since the momenta $\mathbf{k}_{1z}$ and $\mathbf{k}_{2z}$ become correlated through $\phi_1(\mathbf{k}_1 + \mathbf{k}_2)$, this implies that $\langle \mathbf{k}_{1z} \mathbf{k}_{2z} \rangle \neq \langle \mathbf{k}_{1z} \rangle \langle \mathbf{k}_{2z} \rangle = 0$.

III. PARTON CORRELATIONS

We are now ready to investigate the size of the various diparton correlation effects using the bag model dPDFs. We start by studying the dependence of the dPDF $uu(x_1, x_2, \mathbf{k}_\perp)$ on x_1 and $|\mathbf{k}_\perp|$, keeping $x_2 = 0.4$ fixed for simplicity. As the left panel of Fig. 4 shows, the dPDF reduces significantly with increasing $|\mathbf{k}_\perp|$. In the right panel we test the ansatz in Eq. (2) that the dependence on x_i and $\mathbf{k}_\perp$ is uncorrelated, by dividing by $uu(0.4, 0.4, \mathbf{k}_\perp)$. If the ansatz holds, the universal transverse function $G(\mathbf{k}_\perp)$ should drop out in this ratio, making the result independent of $\mathbf{k}_\perp$. As the plot shows, this seems to holds quite well. It only breaks down for the largest values of $|\mathbf{k}_\perp|$, where the dPDF is orders of magnitude smaller than at $|\mathbf{k}_\perp| = 0$. We also note that there is some leakage into the unphysical region $x_1 + x_2 > 1$, as was the case for the single PDF in Fig. 3, though this effect is reasonably small.

Next we explore the x_1, x_2 dependence of dPDF $uu(x_1, x_2, \mathbf{k}_\perp)$ for $\mathbf{k}_\perp = \mathbf{0}$, which is shown in Fig. 5. As x_2 is increased, the peak of the x_1-distribution moves to smaller x_1, responding to the reduced momentum available. The peak height reduces as well, though not for small x_2 since the bag model only describes the valence quarks. To test the factorization ansatz in Eq. (3) for $n = 0$, we divide by $u(x_2)$ in the right panel. Since the resulting distributions clearly still depend on x_2, correlations between x_1 and x_2 are important. Inclusion of the factor of $(1 - x_1 - x_2)^n$ does not alter this conclusion. The correlations can also be seen in the three-dimensional plot of Fig. 6. We remind the reader that this conclusion depends on the treatment of the bag, since x_1 and x_2 would be uncorrelated if a rigid bag was assumed (see Sec. II D).

The relative size of the various spin structures in Sec. II C are studied in Fig. 7. They are shown as a function of x_1 (top row) and $|\mathbf{k}_\perp|$ (bottom row), keeping all other variables fixed. All spin structures show a similar dependence on x_1, though there is a hierarchy between their sizes. The shape of the $|\mathbf{k}_\perp|$ dependence differs between the various spin structures. They all decrease for large $|\mathbf{k}_\perp|$, but $\delta q \delta q^t$ also decreases as $|\mathbf{k}_\perp|$ goes to zero whereas the others are maximal at $|\mathbf{k}_\perp| = 0$. This can be understood because $\delta q \delta q^t$ explicitly requires a transverse scale ($\mathbf{z}_\perp$ or $\mathbf{k}_\perp$) to be defined, so it must vanish at $|\mathbf{k}_\perp| = 0$. These same figures also illustrate the differences between the uu (left column) and ud (right column) dPDF. Unlike the single PDF, where the difference between u and d was simply an overall factor of $n_u/n_d = 2$, the double PDF has more flavor dependence. This arises through the spin dependence and the correlations in the spin-flavor wave function. As Fig. 7 shows, the difference between uu and ud is fairly small. However, the spin correlations are about twice as big for ud than for uu.

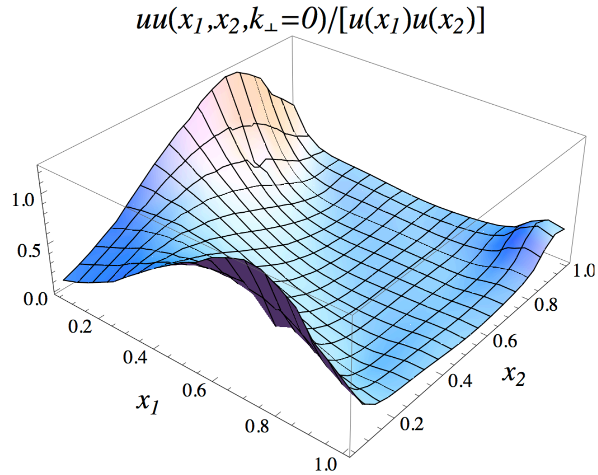

FIG. 6. The correlation between the momentum fractions of two u quarks in the proton is shown by plotting the ratio of the double PDF $uu(x_1, x_2, \mathbf{k}_\perp = 0)$ to the product of two single PDFs $u(x_1)u(x_2)$.

IV. CONCLUSIONS

We have computed the dPDFs using a bag model for the proton. The bag model results should be treated as the dPDFs at a low scale, which can then be evolved to higher energy using the known QCD evolution equations [14, 17]. We find substantial diparton correlations in the proton in spin, flavor, and momentum fraction, which have traditionally been ignored in analyses of double parton scattering, but only a small correlation with the transverse momentum $\mathbf{k}_\perp$. The uu and ud dPDFs are not simply related to each other, or to the single PDFs u and d, because of the spin-flavor correlations in the proton quark model wavefunction in Eq. (7). The results in this paper provide quantitative results for these diparton correlations, which will help in the experimental analysis of double parton scattering at the LHC.

ACKNOWLEDGMENTS

We would like to thank G. Miller and R. Jaffe for helpful discussions. This work is supported in part by DOE grant DE-FG02-90ER40546.

Appendix A

We collect simplified expressions for the bag model wave function in momentum space and the functions ϕ_n needed for the PY projection. Several of these results were already obtained in Ref. [23]. The Fourier transform of the wave function is

$$\begin{aligned} \Psi_m(\mathbf{p}) &= \int \mathrm{d}^3\mathbf{x}\, e^{\mathrm{i}\mathbf{p}\cdot\mathbf{x}}\, \Psi_m(\mathbf{x}) \\ &= \frac{2\pi\Omega R^{3/2}}{\sqrt{\Omega^2 - \sin^2\Omega}} \begin{pmatrix} s_1(\kappa)\chi_m \\ s_2(\kappa)\, \hat{\mathbf{p}}\cdot\boldsymbol{\sigma}\, \chi_m \end{pmatrix}, \end{aligned} \tag{A1}$$

where $\kappa = |\mathbf{p}|R$ and

$$\begin{aligned} s_1(\kappa) &= \frac{1}{\kappa}\Big[\frac{\sin(\kappa - \Omega)}{\kappa - \Omega} - \frac{\sin(\kappa + \Omega)}{\kappa + \Omega}\Big], \\ s_2(\kappa) &= 2 j_0(\Omega) j_1(\kappa) - \frac{\kappa}{\Omega} s_1(\kappa), \end{aligned} \tag{A2}$$

and χ_m is defined in Eq. (5). For the unpolarized and longitudinally polarized single PDFs this leads to

$$\begin{aligned} \bar{\Psi}_m \frac{\not{n}}{2} \Psi_m &= \frac{\pi R^3 \Omega^2}{2(\Omega^2 - \sin^2\Omega)} \left(s_1^2 + s_2^2 + 2 s_1 s_2 \hat{p}^z\right), \\ \bar{\Psi}_m \frac{\not{n}}{2} \gamma_5 \Psi_m &= (-1)^{m+3/2} \frac{\pi R^3 \Omega^2}{2(\Omega^2 - \sin^2\Omega)} \\ &\quad \times [s_1^2 + s_2^2(1 - 2\hat{\mathbf{p}}_\perp^2) + 2 s_1 s_2 \hat{p}^z]. \end{aligned} \tag{A3}$$

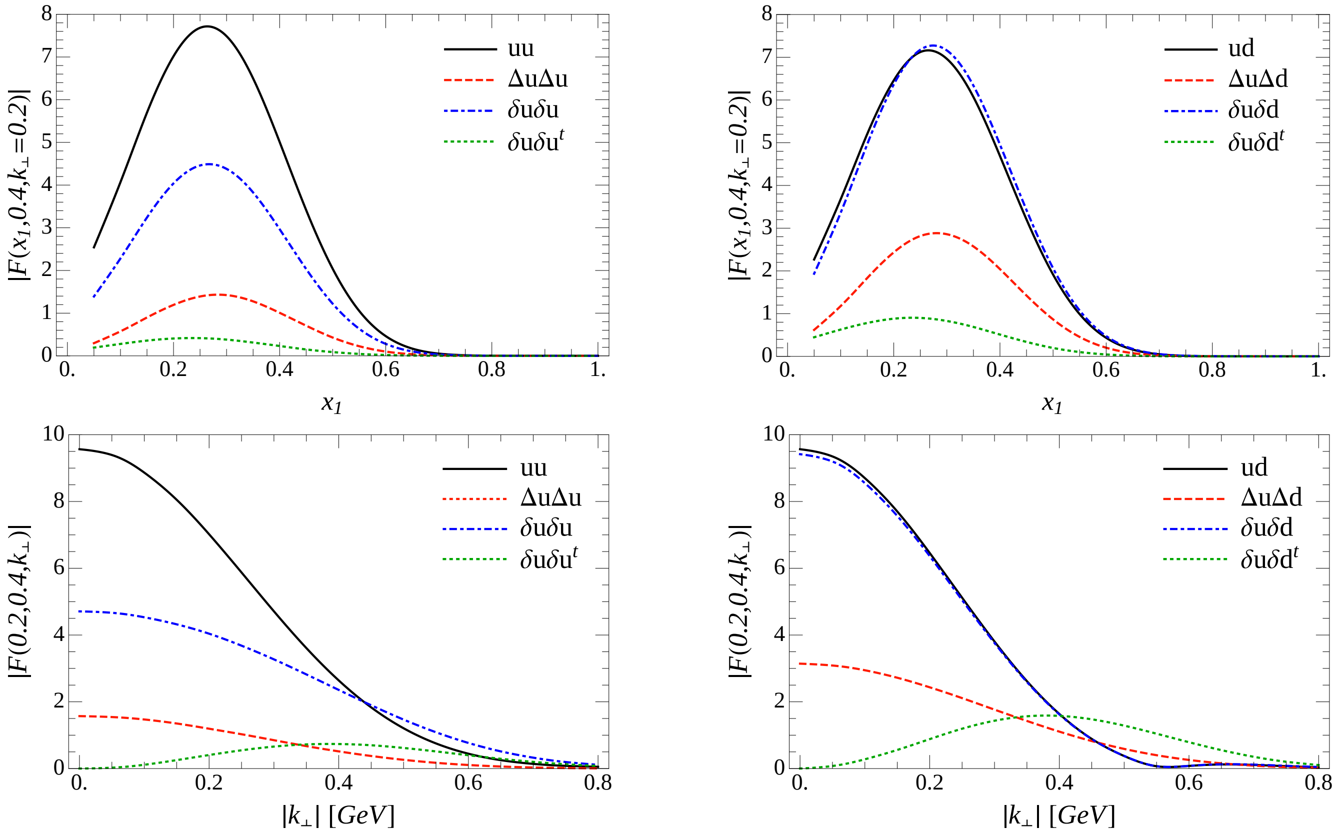

FIG. 7. Comparison of the dPDF spin structures as functions of x_1 or $|\mathbf{k}_\perp|$, keeping the other variable fixed. The left panels show the uu dPDFs, and the right panels show the ud dPDFs. The $\delta u\delta u$, $\delta u\delta u^t$, $\Delta u\Delta d$ and $\delta u\delta d^t$ distributions are negative.

For the transversely polarized PDF we need

$$\bar{\Psi}_\uparrow \frac{\not{n}}{2}\gamma_\perp^\mu\gamma_5\Psi_\downarrow + \bar{\Psi}_\downarrow \frac{\not{n}}{2}\gamma_\perp^\mu\gamma_5\Psi_\uparrow = \frac{\pi R^3\Omega^2}{\Omega^2-\sin^2\Omega}\left[s_1^2+s_2^2(1-\hat{\mathbf{p}}_\perp^2)+2s_1s_2\hat{p}^z\right]. \tag{A4}$$

The functions ϕ_n, used in the PY projection, are

$$|\phi_n(\mathbf{p})|^2 = \frac{2^{4-n}\pi R^3\Omega^{n-2}}{\kappa(\Omega^2-\sin^2\Omega)^n}\int_0^\Omega \frac{dv}{v^{n-1}}\,\sin\frac{2\kappa v}{\Omega}\,T^n(v)\,, \tag{A5}$$

with

$$T(v) = \left(\Omega-\frac{1-\cos 2\Omega}{2\Omega}-v\right)\sin 2v - \left(\frac{1}{2}+\frac{\sin 2\Omega}{2\Omega}\right)\cos 2v + \frac{1}{2}+\frac{\sin 2\Omega}{2\Omega}-\frac{1-\cos 2\Omega}{2\Omega^2}v^2\,. \tag{A6}$$

---

[1] A. Kulesza and W. Stirling, Phys. Lett., **B475**, 168 (2000), arXiv:hep-ph/9912232.

[2] E. Cattaruzza, A. Del Fabbro, and D. Treleani, Phys. Rev., **D72**, 034022 (2005), arXiv:hep-ph/0507052.

[3] E. Maina, JHEP, **0909**, 081 (2009), arXiv:0909.1586 [hep-ph].

[4] J. R. Gaunt, C.-H. Kom, A. Kulesza, and W. Stirling, Eur. Phys. J., **C69**, 53 (2010), arXiv:1003.3953 [hep-ph].

[5] A. Del Fabbro and D. Treleani, Phys. Rev., **D61**, 077502 (2000), arXiv:hep-ph/9911358.

[6] M. Hussein, Nucl. Phys. Proc. Suppl., **174**, 55 (2007), arXiv:hep-ph/0610207.

[7] D. Bandurin, G. Golovanov, and N. Skachkov, JHEP, **1104**, 054 (2011), arXiv:1011.2186 [hep-ph].

[8] E. L. Berger, C. Jackson, S. Quackenbush, and G. Shaughnessy, Phys. Rev., **D84**, 074021 (2011), arXiv:1107.3150 [hep-ph].

[9] ATLAS Collaboration, *A measurement of hard double-partonic interactions in $W \to \ell\nu$ + 2 jet events*, Tech. Rep. ATLAS-CONF-2011-160 (CERN, Geneva, 2011).

[10] N. Paver and D. Treleani, Nuovo Cim., **A70**, 215 (1982).

[11] M. Mekhfi, Phys. Rev., **D32**, 2380 (1985).

[12] M. Diehl and A. Schafer, Phys. Lett., **B698**, 389 (2011), arXiv:1102.3081 [hep-ph].

[13] M. Diehl, D. Ostermeier, and A. Schafer, JHEP, **1203**, 089 (2012), arXiv:1111.0910 [hep-ph].

[14] A. V. Manohar and W. J. Waalewijn, Phys. Rev., **D85**, 114009 (2012), arXiv:1202.3794 [hep-ph].

[15] R. Kirschner, Phys. Lett., **B84**, 266 (1979).

[16] V. Shelest, A. Snigirev, and G. Zinovev, Phys. Lett., **B113**, 325 (1982).

[17] A. V. Manohar and W. J. Waalewijn, Phys. Lett., **B713**, 196 (2012), arXiv:1202.5034 [hep-ph].

[18] M. Mekhfi and X. Artru, Phys. Rev., **D37**, 2618 (1988).

[19] T. Kasemets and M. Diehl, arXiv:1210.5434 [hep-ph].

[20] A. Chodos, R. Jaffe, K. Johnson, and C. B. Thorn, Phys. Rev., **D10**, 2599 (1974).

[21] R. Jaffe, Phys. Rev., **D11**, 1953 (1975).

[22] C. Benesh and G. Miller, Phys. Rev., **D36**, 1344 (1987).

[23] A. W. Schreiber, A. Signal, and A. W. Thomas, Phys. Rev., **D44**, 2653 (1991).

[24] X.-M. Wang, X.-T. Song, and P.-C. Yin, Hadronic J., **6**, 985 (1983).

[25] J. R. Gaunt and W. J. Stirling, JHEP, **03**, 005 (2010), arXiv:0910.4347 [hep-ph].

[26] A. V. Manohar, Phys. Rev., **D70**, 014004 (2004), arXiv:hep-ph/0404122.

[27] R. Peierls and J. Yoccoz, Proc. Phys. Soc., **A70**, 381 (1957).

[28] F. E. Close and A. W. Thomas, Phys. Lett., **B212**, 227 (1988).

[29] T. Hahn, Comput. Phys. Commun., **168**, 78 (2005), arXiv:hep-ph/0404043.